VIP DNA Nanocages Very Important Paper

Deutsche Ausgabe: DOI: 10.1002/ange.201500755
Internationale Ausgabe: DOI: 10.1002/anie.201500755

Structural Transformation: Assembly of an Otherwise Inaccessible DNA Nanocage**

*Yulin Li, Cheng Tian, Zhiyu Liu, Wen Jiang, and Chengde Mao**

Abstract: *A strategy of structural transformation for the assembly of DNA nanocages that can not be assembled directly is described. In this strategy, a precursor DNA nanocage is assembled first and then is isothermally transformed into a desired, complicated nanocage. A dramatic, conformational change accompanies the transformation. This strategy has been proven to be successful by native polyacrylamide gel electrophoresis (PAGE) and cryogenic electron microscopy (cryoEM) imaging. We expect that the strategy of structural transformation will be useful for the assembly of many otherwise inaccessible DNA nanostructures and help to increase the structural complexity of DNA nanocages.*

In last three decades, great effort has been made regarding the construction and application of DNA nanostructures,[1–3] including various DNA nanocages.[4–16] Such nanocages promise applications for cargo encapsulation,[17–19] 3D protein/nanoparticle organization,[20,21] controlled nano-object delivery,[18,22,23] etc. Structural control of the nanocages is key to fully meet those potentials. Research activity in the field is constantly updating on two fronts: the structural complexity that can be achieved and how complex structures can be assembled in a simple way. It has been demonstrated that the shape and surface porosity of a DNA nanocage could be reversibly switched.[12,14,24,25] In most cases, the structural changes/reconfigurations can be easily predicted and both the starting/ending structures could be assembled directly. Herein, we have applied structural transformation as a way to assemble complex DNA nanocages that cannot be assembled directly. During the transformation, there is a dramatic conformational change that is not easily predicted.

Structural transformation between three DNA nanocages has been realized by isothermal strand displacement (Figure 1).[26] We start with a triakis tetrahedron (cage **I**),[10] a multicavity nanocage that can be directly assembled from a six-point-star motif (M^6_A) and a three-point-star motif (M^3). All the branches of the motifs have sticky ends on the outside

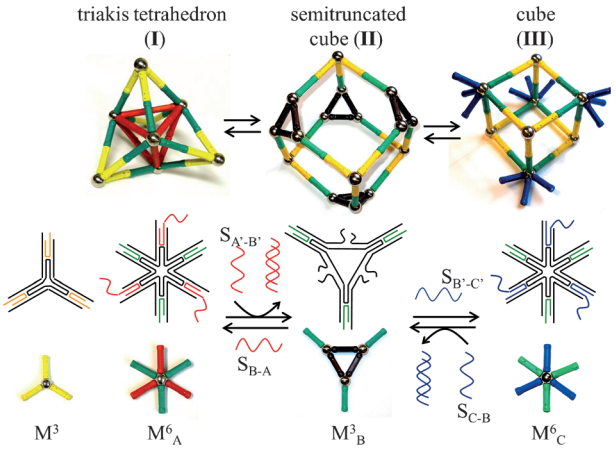

Figure 1. Structural transformation of DNA nanocages. Top panel: DNA nanocages; bottom panel: corresponding component DNA nanomotifs and their simple rod-ball representations. Each line in the motif structure represents a DNA strand and each rod represents one branch (two interconnected, parallel DNA duplexes) of the motifs. Three arms (red rods) of motif M^6_A can self-associate while the other three arms (green rods) can only associate with the arms (yellow rods) of motif M^3. Structural transformation is realized by specific addition or removal of a DNA strand from the 6-point-star motifs M^6_A and M^6_C by toe-hold-mediated strand displacement. Note that during the whole process, there is no change to motif M^3 or the association between the yellow arms and the green arms.

for further assembly. Three branches of M^6_A can self-associate to form the central tetrahedral chamber and the other three branches can associate with M^3 motifs to produce four tetrahedral chambers outside of the four faces of the central tetrahedron. All the tetrahedral chambers have the same edge length: four helical turns or approximately 14 nm. there is a 10-nucleotide (nt) long, single-stranded overhang on strand $S_{B\text{-}A}$ at the end of each self-associating arm in M^6_A in the assembled cage **I**. The structural transformation is triggered by the addition of a DNA strand $S_{A'\text{-}B'}$, which is fully complementary to $S_{B\text{-}A}$. It binds to strand $S_{B\text{-}A}$ at the overhang region and gradually displaces it from cage **I** to form a short duplex, $S_{A'\text{-}B'}/S_{B\text{-}A}$. After the removal of strand $S_{B\text{-}A}$, the original M^6_A motif becomes a pseudo-three-point-star motif M^3_B, which has an open triangle in the center. Accordingly, the original cage **I** becomes a structure with a single cavity. It resembles a cube, but has four open vertexes. We named it a semitruncated cube (cage **II**). This step of the transformation process can be reversed by re-introduction of strand $S_{B\text{-}A}$. To further close the four open vertexes, we can add strand $S_{B'\text{-}C'}$, which can not self-associate to define an inner chamber, but is able to change M^3_B into a new six-arm motif M^6_C. As

[*] Dr. Y. Li, Dr. C. Tian, Z. Liu, Prof. C. Mao
Department of Chemistry, Purdue University
West Lafayette, IN 47907 (USA)
E-mail: mao@purdue.edu
Prof. W. Jiang
Markey Center for Structural Biology and
Department of Biological Sciences, Purdue University
West Lafayette, IN 47907 (USA)

[**] We would like to thank the Office of Nava Research and the National Science Foundation for supporting this work.

Supporting information for this article is available on the WWW under http://dx.doi.org/10.1002/anie.201500755.

a result, cage **II** is converted into cage **III**, a new single-cavity cube with closed vertexes. As a consequence of the overhang domain of strand $S_{B'-C'}$, cage **III** can also be reversibly transformed into cage **II** by strand displacement (displacing strand $S_{B'-C'}$ with a strand S_{C-B}; these two stands are fully complementary to each other).

Cage **I** has been directly self-assembled before[10] and cage **III** is expected to be able to self-assemble because both component motifs are highly structured. However, cage **II** could not self-assemble from its component motifs (M^3 and M^3_B). Motif M^3_B is poorly structured. At the center of the motif, there is an equilateral triangle. Each side contains two 5-base-long (TTTTT) single-stranded bulges and two single-stranded tails, which make the motif very flexible. Direct assembly of M^3 and M^3_B would produce a series of complexes with different molecular weights, but the dominant product is expected to be the smallest complex, a heterodimer of M^3 and M^3_B. Thus, preparing cage **II** is a challenge. Here we propose that we can prepare cage **I** or **III** first, and then convert them into cage **II** through structural transformation, as outlined in Figure 1.

First, we examined the direct assembly of the three nanocages from the component DNA tiles by native PAGE (Figure 2). For cages **I** and **III**, dominant, sharp bands

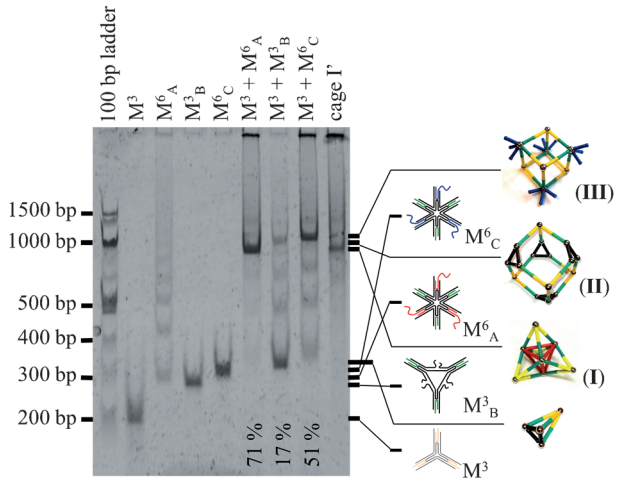

Figure 2. Native polyacrylamide gel electrophoretic (PAGE) analysis of the direct self-assembly of DNA nanocages from component motifs. Cage **I′** is a previously reported triakis tetrahedron (TET), but without single-stranded overhangs on strand S_{B-A}. It serves as a size marker. The sample composition in each lane and the chemical identity of each band are indicated above and beside the gel image, respectively. The assembly yield of each cage has been estimated on the basis of the band intensity by ImageJ, an image processing software, and shown at the bottom of the corresponding lane.

appeared in the lanes corresponding to the two samples. The band for cage **I** (a triakis tetrahedron with twelve 10-base-long overhangs) migrated the same as a previously reported triakis tetrahedron without extended overhangs (cage **I′**). As the two cages had the same 3D structures and similar molecular weights (3324 nucleotides for cage **I** and 3204 nucleotides for cage **I′**), similar mobilities were expected. Cage **III** migrated significantly slower as it was much less compact than cage **I**. The PAGE experiment suggested that cages **I** and **III** assembled successfully, as designed. However, the assembly was different for cage **II**. A band corresponding to cage **II** appeared. It migrated much slower than cage **I** because cage **I** was more compact, and migrated slightly faster than cage **III** because cage **III** had a slightly higher molecular weight. The band was very weak. Besides the desired band, multiple, high-mobility (low-molecular-weight) bands existed. The major band had a quite low molecular weight (high mobility), which was presumably a heterodimer of motifs M^3_B and M^3. This observation indicated that the direct assembly of cage **II** failed. It was not a surprise because M^3_B was very flexible. Note that in the lane of M^6_A, there are a series of bands, which are oligo-M^6_A complexes formed through the interaction between the self-associating arms.

Although direct assembly worked poorly for cage **II**, structural transformation provided an effective way to prepare it (Figure 3 and see Figure S2 in the Supporting

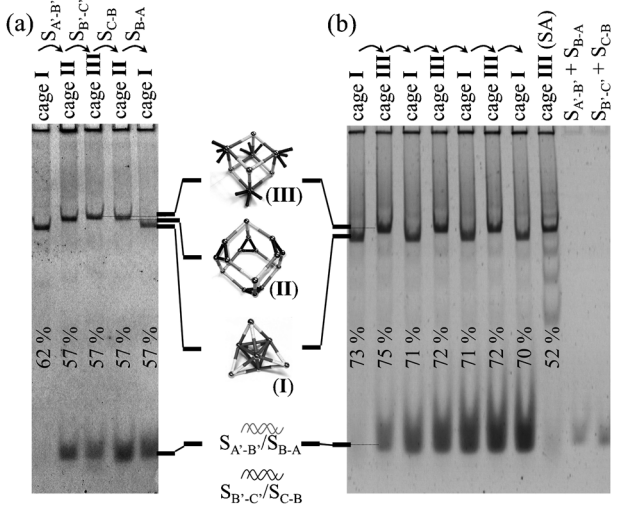

Figure 3. Reversible transformation process demonstrated by native PAGE. a) One complete cycle of the transformation: cage **I**→**II**→**III**→**II**→**I**. b) Multiple cycles of the structural transformation. The sample composition in each lane and the chemical identity of each band are indicated above and beside the gel images, respectively. The yields are shown in the corresponding lanes. The arrows above the gel indicate the transformation process. The sample "cage **III** (SA)" was prepared by direct self-assembly from motifs M^3 and M^6_C and used as a control.

Information). The structural transformation was demonstrated by native PAGE (Figure 3a). Cage **I** was assembled directly from the component motifs. Upon addition of strand $S_{A'-B'}$, strand S_{B-A} would be removed from cage **I**, which consequently became cage **II**, as shown schematically in Figure 1. The transformation from cage **I** to cage **II** was evidenced by a significant shift in the electrophoretic mobility and the appearance of a new high-mobility band corresponding to the waste duplex of $S_{A'-B'}/S_{B-A}$. The transformation was near quantitative, as the original band of cage **I** completely disappeared. When another strand $S_{B'-C'}$ was added, cage **II** was further converted into cage **III**, thereby resulting in

a small mobility shift. The whole process could be reversed from cage **III** to cage **II** (by adding strand $S_{C\text{-}B}$), and then back to cage **I** (by adding strand $S_{B\text{-}A}$). Thus, cage **II** could be prepared in high yield by structural transformation from cage **I** or **III**. The transformation was efficient and remarkably robust. The above described process could be repeated for multiple cycles (Figure 3b see Figure S2 in the Supporting Information). The samples in different cycles behaved very similar to each other in native PAGE. As the process continued, the waste duplex was accumulated and the intensity of the corresponding band became stronger and stronger.

To directly prove that the 3D structures of the nanocages were as designed, we characterized the cages by cryoEM (Figure 4), which has been proven to be well-suited for the structural study of 3D DNA nanostructures.[4,6,27] Framework-like nanoparticles were randomly distributed in the cryoEM images (Figure 4a,d,g, see Figures S3, S5, and S7 in the Supporting Information). From the observed nanoparticles, we applied a single-particle 3D reconstruction technique[28] to reveal the native 3D structures. This process resulted in a triakis tetrahedron for cage **I** (at a resolution of 4.0 nm), a semitruncated cube structure for cage **II** (at a resolution of 4.8 nm), and a cube structure for cage **III** (at a resolution of 5.1 nm) as expected. To validate the reconstructed structural models, we made pairwise comparisons between the experimentally observed, individual, particle images and computer-generated 2D projections of the reconstructed structural models (Figure 4c,f,i). They clearly matched with each other, thus indicating that the reconstructed models were indeed the native 3D structures of the nanocages. Cages **II** and **III** were similar to each other and exhibited cube-like structures, but clear differences existed. For cage **II**, four vertices were solid (corresponding to motif M^3) and each of the other four had one triangle-shaped opening (corresponding to the triangle in motif $M^3{}_B$). For cage **III**, all the vertices were solid, but four had lower densities (corresponding to motif M^3) than the other four (corresponding to motif $M^6{}_C$). Cages **II** and **III** were both loosely packed compared to the densely packed cage **I** structure (Figure 4b).

In summary, we have demonstrated that structural transformation can be used to prepare a DNA nanocage that cannot be assembled directly from its component tiles. Accompanying the transformation, there are dramatic changes in the 3D structures and topologies. To the best of our knowledge, there is only one study in the literature that reports a dramatic, but not easily predicted structural change resulting from strand displacement. In that study, a Mobius strip becomes a two-circle catenane and many different removal strands are required.[29] We expect that such a structural transformation will become a general method to prepare complex DNA nanostructures that are not otherwise accessible.

Keywords: DNA nanocages · DNA structures · self-assembly · strand displacement

How to cite: *Angew. Chem. Int. Ed.* **2015**, *54*, 5990–5993
Angew. Chem. **2015**, *127*, 6088–6091

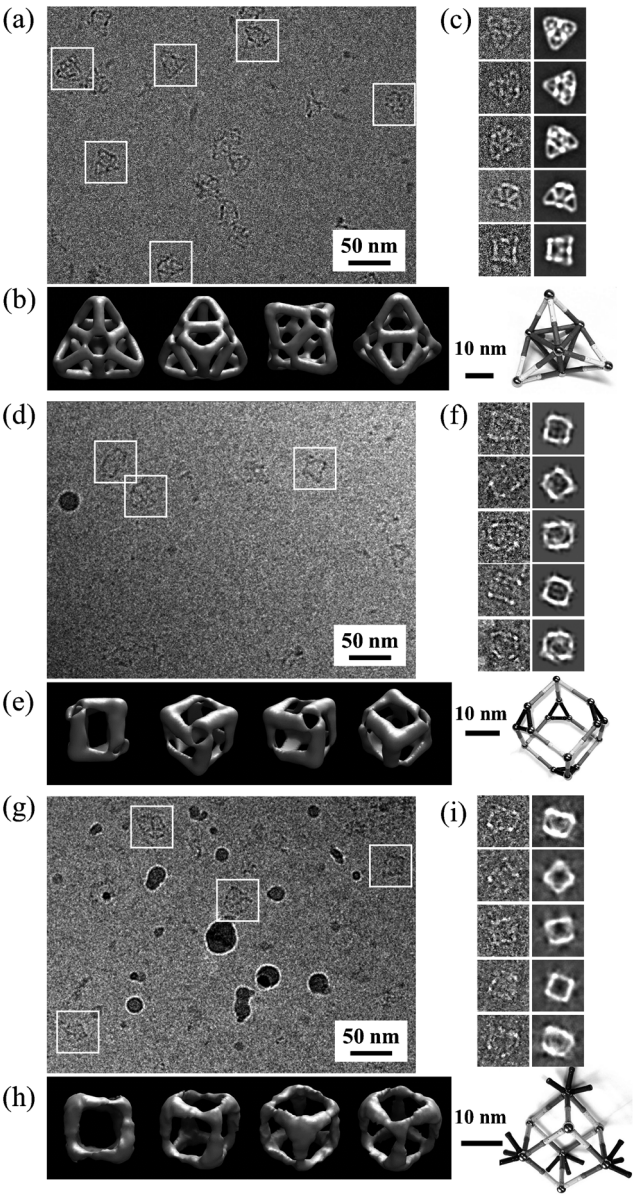

Figure 4. Cryogenic electron microscopy (cryoEM) characterization of cages **I** (a–c), **II** (d–f), and **III** (g–i). a,d,g) Representative cryoEM images. b,e,h) Four views of the reconstructed structural models and the corresponding structural schemes. c,f,i) Pairwise comparison between the raw cryoEM images (left) of individual DNA complexes and the 2D projections (right) back calculated from the reconstructed 3D models.

[1] N. C. Seeman, *Nature* **2003**, *421*, 427–431.
[2] F. A. Aldaye, A. L. Palmer, H. F. Sleiman, *Science* **2008**, *321*, 1795–1799.
[3] F. Zhang, J. Nangreave, Y. Liu, H. Yan, *J. Am. Chem. Soc.* **2014**, *136*, 11198–11211.
[4] W. M. Shih, J. D. Quispe, G. F. Joyce, *Nature* **2004**, *427*, 618–621.
[5] R. P. Goodman, I. A. T. Schaap, C. F. Tardin, C. M. Erben, R. M. Berry, C. F. Schmidt, A. J. Turberfield, *Science* **2005**, *310*, 1661–1665.
[6] Y. He, T. Ye, M. Su, C. Zhang, A. E. Ribbe, W. Jiang, C. Mao, *Nature* **2008**, *452*, 198–201.

[7] C. Zhang, M. Su, Y. He, X. Zhao, P. Fang, A. E. Ribbe, W. Jiang, C. Mao, *Proc. Natl. Acad. Sci. USA* **2008**, *105*, 10665 – 10669.
[8] C. Zhang, S. H. Ko, M. Su, Y. Leng, A. E. Ribbe, W. Jiang, C. Mao, *J. Am. Chem. Soc.* **2009**, *131*, 1413 – 1415.
[9] Y. He, M. Su, P. Fang, C. Zhang, A. E. Ribbe, W. Jiang, C. Mao, *Angew. Chem. Int. Ed.* **2010**, *49*, 748 – 751; *Angew. Chem.* **2010**, *122*, 760 – 763.
[10] C. Tian, X. Li, Z. Liu, W. Jiang, G. Wang, C. Mao, *Angew. Chem. Int. Ed.* **2014**, *53*, 8041 – 8044; *Angew. Chem.* **2014**, *126*, 8179 – 8182.
[11] D. Bhatia, S. Mehtab, R. Krishnan, S. S. Indi, A. Basu, Y. Krishnan, *Angew. Chem. Int. Ed.* **2009**, *48*, 4134 – 4137; *Angew. Chem.* **2009**, *121*, 4198 – 4201.
[12] F. A. Aldaye, H. F. Sleiman, *J. Am. Chem. Soc.* **2007**, *129*, 13376 – 13377.
[13] H. Yang, C. K. Mclaughlin, F. A. Aldaye, G. D. Hamblin, A. Z. Rys, I. Rouiller, H. F. Sleiman, *Nat. Chem.* **2009**, *1*, 390 – 396.
[14] E. S. Andersen, M. Dong, M. M. Nielsen, K. Jahn, R. Subramani, W. Mamdouh, M. M. Golas, B. Sander, H. Stark, C. L. P. Oliveira, J. S. Pedersen, V. Birkedal, F. Besenbacher, K. V. Gothelf, J. Kjems, *Nature* **2009**, *459*, 73 – 76.
[15] Y. Ke, J. Sharma, M. Liu, K. Jahn, Y. Liu, H. Yan, *Nano Lett.* **2009**, *9*, 2445 – 2447.
[16] R. Iinuma, Y. Ke, R. Jungmann, T. Schlichthaerle, J. B. Woehrstein, P. Yin, *Science* **2014**, *344*, 65 – 69.
[17] C. Zhang, X. Li, C. Tian, G. Yu, Y. Li, W. Jiang, C. Mao, *ACS Nano* **2014**, *8*, 1130 – 1135.
[18] P. K. Lo, P. Karam, F. A. Aldaye, C. K. Mclaughlin, G. D. Hamblin, G. Cosa, H. F. Sleiman, *Nat. Chem.* **2010**, *2*, 319 – 328.
[19] C. M. Erben, R. P. Goodman, A. J. Turberfield, *Angew. Chem. Int. Ed.* **2006**, *45*, 7414 – 7417; *Angew. Chem.* **2006**, *118*, 7574 – 7577.
[20] N. Y. Wong, C. Zhang, L. H. Tan, Y. Lu, *Small* **2011**, *7*, 1427 – 1430.
[21] C. Zhang, C. Tian, F. Guo, Z. Liu, W. Jiang, C. Mao, *Angew. Chem. Int. Ed.* **2012**, *51*, 3382 – 3385; *Angew. Chem.* **2012**, *124*, 3438 – 3441.
[22] S. M. Douglas, I. Bachelet, G. M. Church, *Science* **2012**, *335*, 831 – 834.
[23] H. Lee, A. K. R. Lytton-Jean, Y. Chen, K. T. Love, A. I. Park, E. D. Karagiannis, A. Sehgal, W. Querbes, C. S. Zurenko, M. Jayaraman, C. G. Peng, K. Charisse, A. Borodovsky, M. Manoharan, J. S. Donahoe, J. Truelove, M. Nahrendorf, R. Langer, D. G. Anderson, *Nat. Nanotechnol.* **2012**, *7*, 389 – 393.
[24] R. P. Goodman, M. Heilemann, S. Doose, C. M. Erben, A. N. Kapanidis, A. J. Turberfield, *Nat. Nanotechnol.* **2008**, *3*, 93 – 96.
[25] C. Zhang, C. Tian, X. Li, H. Qian, C. Hao, W. Jiang, C. Mao, *J. Am. Chem. Soc.* **2012**, *134*, 11998 – 12001.
[26] B. Yurke, A. J. Turberfield, A. P. Mills, Jr., F. C. Simmel, J. L. Neumann, *Nature* **2000**, *406*, 605 – 608.
[27] X. Bai, T. G. Martin, S. H. W. Scheres, H. Dietz, *Proc. Natl. Acad. Sci. USA* **2012**, *109*, 20012 – 20017.
[28] G. Tang, L. Peng, P. R. Baldwin, D. S. Mann, W. Jiang, I. Rees, S. J. Ludtke, *J. Struct. Biol.* **2007**, *157*, 38 – 46.
[29] D. Han, S. Pal, Y. Liu, H. Yan, *Nat. Nanotechnol.* **2010**, *5*, 712 – 717.

Received: January 26, 2015
Published online: March 25, 2015

